

Supporting Information

Safavi et al. 10.1073/pnas.1802356115

SI Experimental Procedures

In the anesthetized experiment, the animals were initially premedicated with glycopyrrolate (0.01 mg per kg of body weight, i.m.) and ketamine (15 mg/kg, i.m.). Next, an i.v. catheter was inserted, and vital monitors (HP OmniCare/CMS; Hewlett Packard; electrocardiogram, noninvasive blood pressure, CO₂, SpO₂, and temperature) were connected. The monkeys were preoxygenated, and anesthesia was induced with fentanyl (3 µg/kg), thiopental (5 mg/kg), and succinylcholine chloride (3 mg/kg) for the intubation of the trachea. The animals were ventilated by using an Ohmeda anesthesia machine (Ohmeda), maintaining an end-tidal CO₂ of 33 mmHg and oxygen saturation >95%. Balanced anesthesia was maintained with remifentanyl (typical, 1 µg/kg per min). Mivacurium

(5 mg/kg per hour) was used for muscle relaxation. Body temperature was kept constant, and lactated Ringer's solution was given at a rate of 10 mL/kg per hour. During the entire experiment, the vital signs of the monkey and the depth of anesthesia were continuously monitored.

Drops of 1% ophthalmic solution of anticholinergic cyclopentolate hydrochloride were given to each eye to prevent accommodation of the lens and dilation of the pupil. Refractive errors were measured, and contact lenses [hard poly(methyl methacrylate) lenses; Wöhlk] were put on the monkey's eyes with continuous drops of saline throughout the experiment to prevent the eyes from drying. The lenses with the appropriate dioptric power were used to bring the animal's eyes into focus on the stimulus plane.

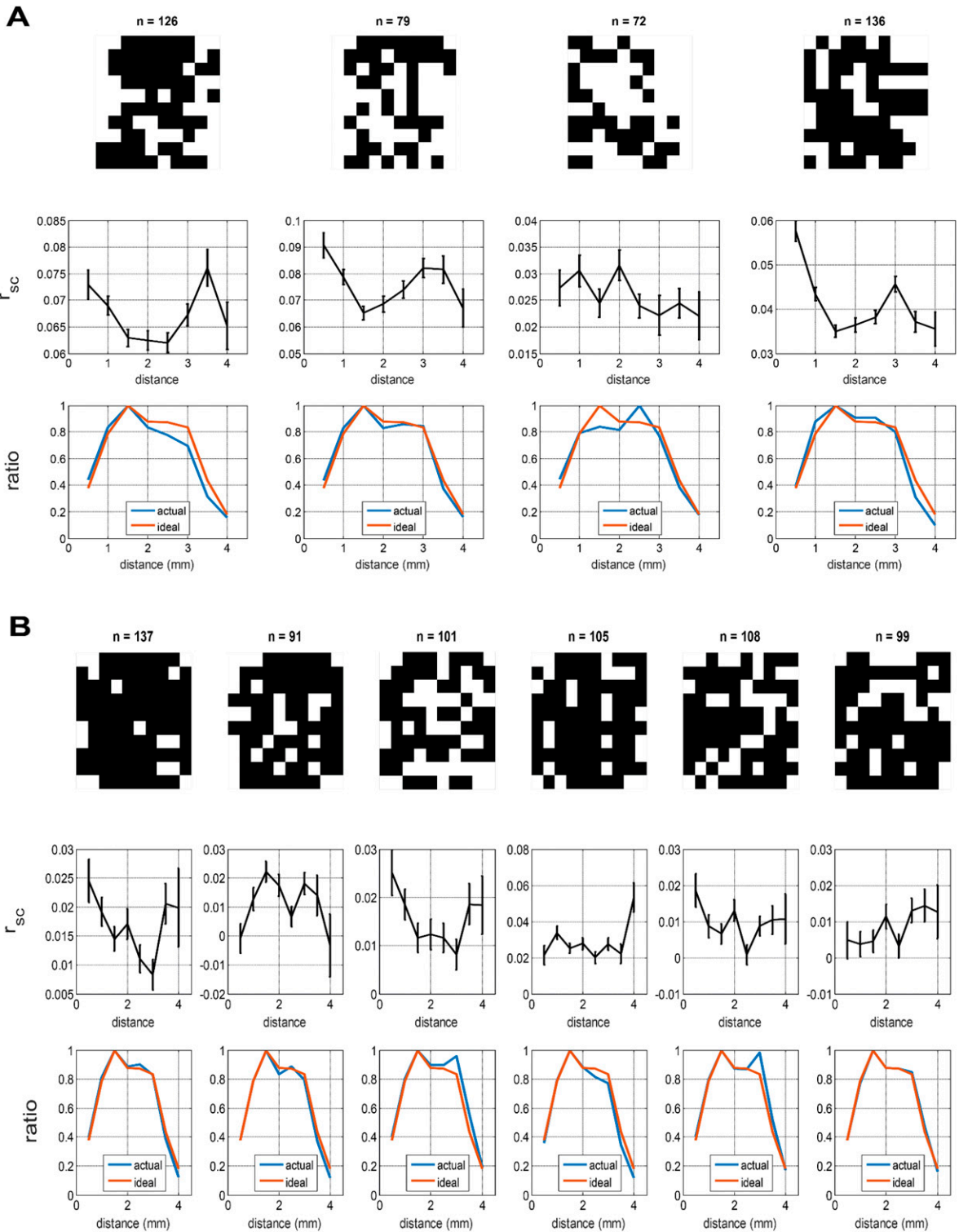


Fig. S1. Related to Fig. 2: Spatial distribution of single units in anesthetized- and awake-state recordings. (A) *Top* depicts the spatial coverage of the detected single units (n) on the Utah array (10×10 array of electrodes) for four individual datasets from the anesthetized recordings (each column corresponds to an individual dataset). Black pixels indicate channels where at least one single unit was detected. In *Middle*, similar to Fig. 2, correlated variability is depicted as a function of distance during visual stimulation for the same datasets. In *Bottom*, we plot the spatial distributions of the recorded pairs as a function of distance on the Utah arrays (actual) for individual datasets. To test if the spatial structure of spike count correlations was an artifactual reflection of the spatial distribution of isolated neurons in our recordings, we compared the actual distribution of the pairs with an “ideal” distribution across distance bins. This ideal distribution is derived from a simulated dataset where we could detect an equal number of neurons on all sites, indicating the best possible sampling one can achieve with the Utah arrays. To simulate this ideal distribution, we considered a maximum number of detected single neurons on all sites and found the distribution of pairs (aka *ideal* distribution). The largest number of single units among all sites in the recorded dataset was used as the maximum number. For example, if in a given dataset, n single units were the largest number of single units across all electrodes, we considered a distribution derived from n single units across all sites. The choice of this maximum is not crucial, as distributions are normalized. Blue and orange traces indicate the actual and ideal distribution of number of pairs (normalized to the peak) in four datasets across all distance bins. The spatial spread of the recorded single units is not significantly different from an ideal distribution. (B) Similar to A, but for awake-state datasets.

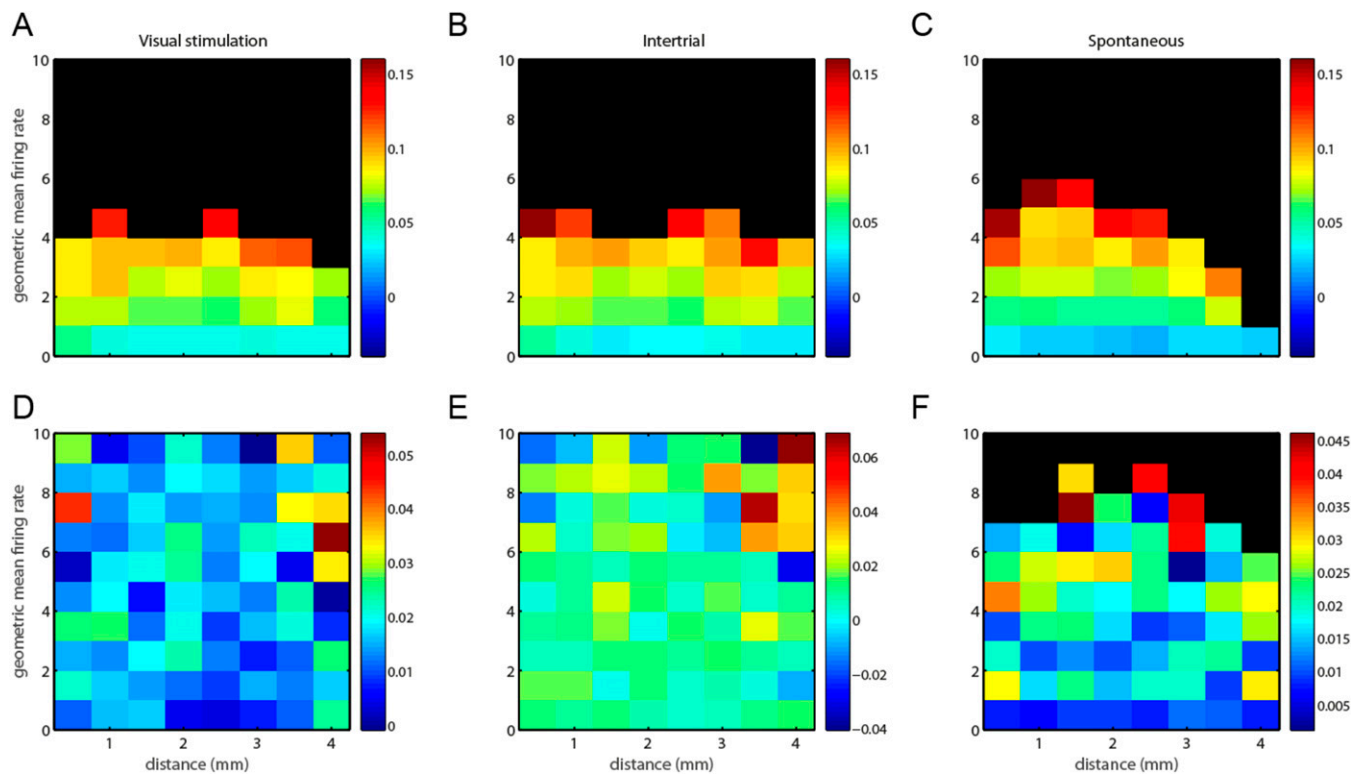


Fig. S3. Related to Fig. 2: Correlated variability as a function of distance for populations with matched geometric mean firing rates. To control for spatial variations in firing rates giving rise to the nonmonotonic structure of correlated variability, we plot correlated variability as a function of distance and geometric mean of the firing rates during different states and conditions: anesthetized, visual stimulation (A), intertrial (B), and spontaneous activity (C); and awake, visual stimulation (D), intertrial (E), and spontaneous activity (F). The color of each pixel indicates the average correlated variability for pairs whose geometric mean firing rate and distance landed in the specific bin. Therefore, each row contains pairs with similar firing rate geometric mean. Pixels containing <10 pairs were removed (black pixels). Correlated variability values are indicated by the color bar at the right of the panel. Data were not smoothed.

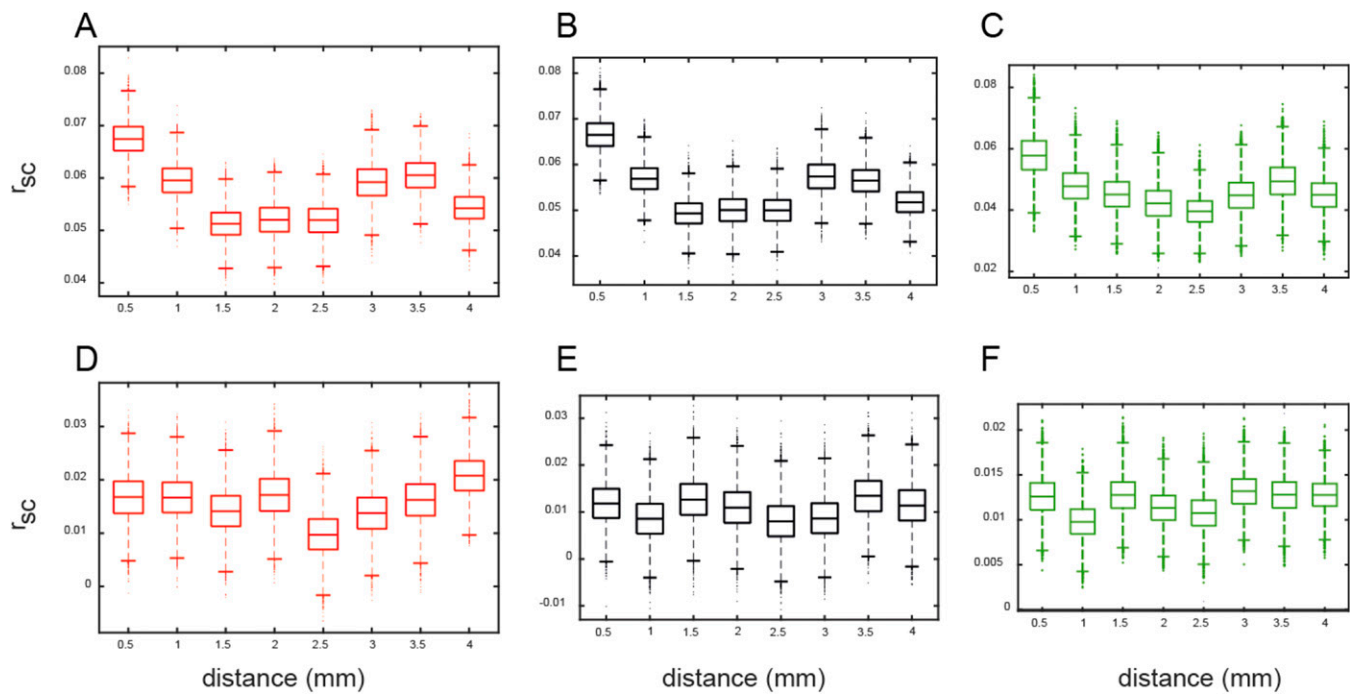


Fig. S4. Related to Fig. 2: Bootstrapping for the spatial sampling. To control for whether the intrinsic nonuniformity of spatial sampling with Utah array influences the nonmonotonic structure of correlated variability, we used a bootstrap analysis for different states and conditions: anesthetized, visual stimulation (A), intertrial (B), and spontaneous activity (C); and awake, visual stimulation (D), intertrial (E), and spontaneous activity (F). Each image depicts the box-plot of the mean of the thus-derived pseudodatasets across all distance bins. For each state-condition, we bootstrapped 10,000 times. We obtained a set of G ($=10,000$) draws from the distribution of all pairs belong to a particular distance bin. For each draw, we constructed a pseudodataset where the size of each pseudodataset is limited by the sample size of the distance bin that contains the least number of pairs. Therefore, all distance bins contain an equal number of samples in any draw (usually the largest distance bin, i.e., 3.75–4.25 mm). This analysis suggests that the equalized resampling of the pairs across distance bins show similar results (Fig. 2). Therefore, the nonmonotonic structure in correlated variability could not be ascribed to the nonuniformity of the spatial sampling of the Utah arrays.

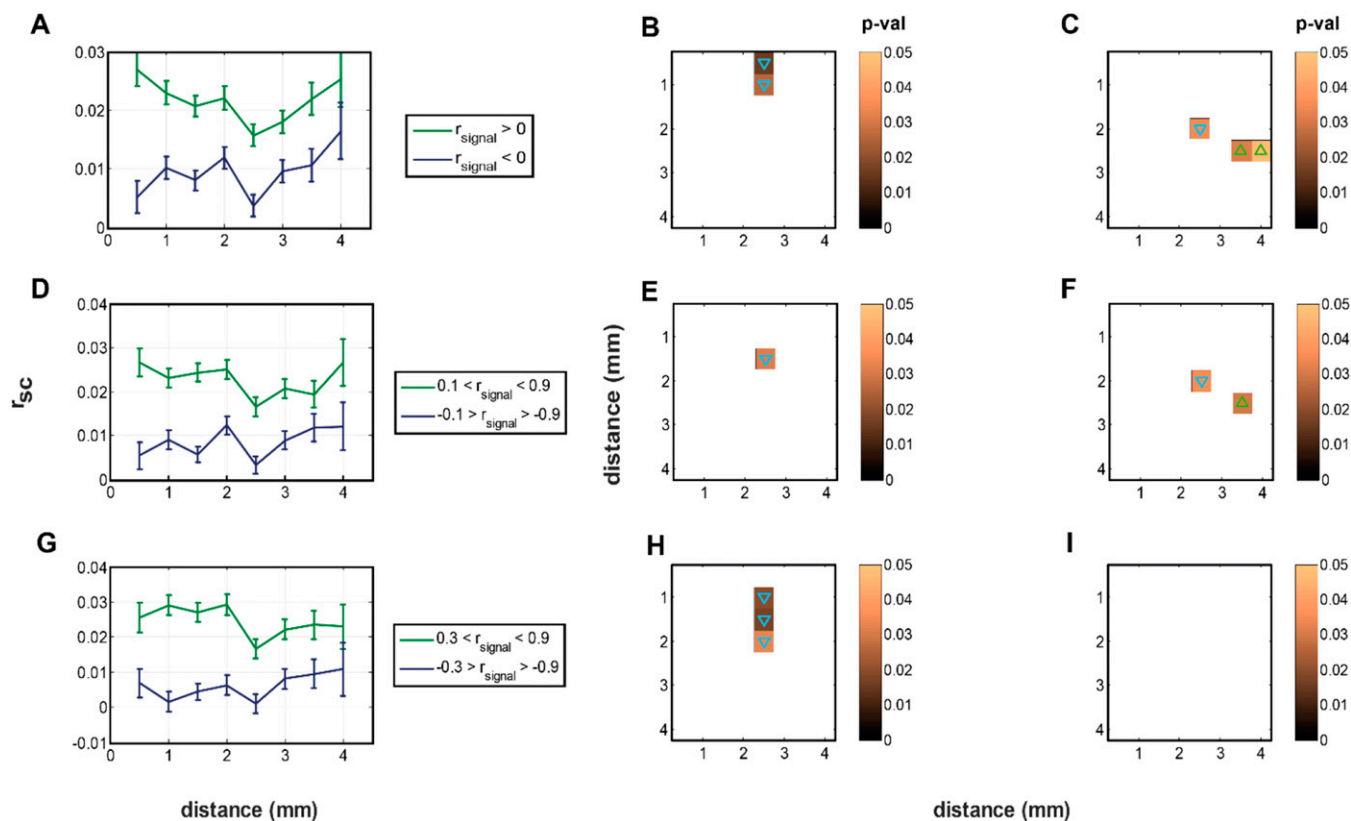


Fig. S5. Related to Fig. 6: Various thresholds of signal correlation. (A–C) Correlation as a function of distance for different thresholds of signal correlation (similar to Fig. 6B): Pairs with positive signal correlations are depicted in green (A, $r_{\text{signal}} > 0$; B, $0.1 < r_{\text{signal}} < 0.9$; C, $0.3 < r_{\text{signal}} < 0.9$), and negative signal correlations are depicted in blue (A, $r_{\text{signal}} < 0$; B, $-0.9 < r_{\text{signal}} < -0.1$; C, $-0.9 < r_{\text{signal}} < -0.3$; mean value \pm SEM as error bars). (D, F, and H) Similar to the matrix plots in Fig. S2, but for different ranges of positive signal correlations (green curves) depicted in A–C. Each plot depicts the statistical significance (based on the Wilcoxon rank-sum test) of differences in correlations, across all possible pairwise distance bin comparisons. (E, G, and I) Similar to D, F, and H but for negative signal correlations (blue curves) depicted in A–C.

Table S1. Related to Fig. 2: Summary of *P* values in the anesthetized state for comparison of correlated variability in three key distance bins mentioned in the main text, viz 0.5, 2.5, and 3.5 mm

Distance bins, mm	Bonferroni adjusted alpha	Visual stimulation all pairs (Fig. 2B, red)
0.5 vs. 2.5	0.0167	$<10^{-10}$
2.5 vs. 3.5	0.0167	0.004
0.5 vs. 3.5	0.0167	0.0008

Table S2. Related to Fig. 2: Summary of *P* values in the awake state for comparison of correlated variability in three key distance bins mentioned in the main text. (1 mm during visual stimulation and 0.5 mm during intertrial and spontaneous states)

Distance bins, mm	Bonferroni adjusted alpha	Visual stimulation all pairs (Fig. 2B, red)	Intertrial all pairs (Fig. 2B, black)	Spontaneous all pairs (Fig. 2B, dark blue)
0.5 or 1.0 vs. 2.5	0.0167	0.0038	0.3	0.6
2.5 vs. 4.0	0.0167	0.0079	0.25	>0.1
0.5 or 1.0 vs. 4.0	0.0167	>0.3	0.8	0.33

